Multi-lithology stratigraphic model under maximum erosion rate constraint

R. Eymard[‡] T. Gallouët[§] D. Granjeon[†]
R. Masson[†] Q.H. Tran[†]

March 23, 2011

Abstract

Non-linear single lithology or multi-lithology diffusion models have been widely used by sedimentologists and geomorphologists in the field of stratigraphic basin simulations to simulate the large scale depositional transport processes of sediments. Nevertheless, as noticed by many authors, erosion and sedimentation processes are non symmetric. Soil material must first be produced in situ by weathering processes prior to be transported by diffusion. This is usually taken into account through a prescribed maximum erosion rate of the sediments, but no mathematical description of the coupling with the diffusion model has been proposed so far. In this paper, we introduce a new mathematical formulation for the coupling of the weather limited erosion and the multi-lithology diffusion models, which appears as a non standard free boundary problem for a new variable acting as a limitor of the fluxes.

One of the main advantages of this formulation, compared to existing discrete coupling models, is to enable the definition of efficient discretization schemes. A finite volume scheme with implicit time integration is introduced which is proved to be unconditionally stable in the l^∞ norm for the sediment thickness, the sediment concentrations in the lithologies, and the flux limitor variables. A Newton algorithm with an iterative computation of the saturated constraints is used to solve efficiently the non-linear system resulting from the discretization. The efficiency of the model and the numerical scheme is illustrated on 2D and 3D basin simulation examples.

1 Introduction

In recent years, there has been a growing interest in the development of mathematical and numerical models in stratigraphy and sedimentology in response to the need for quantitative modeling in a traditionally qualitative science. In the field of sequence stratigraphy, forward numerical models have shown to be useful tools to study the effects of eustasy, tectonics, and sediment supply on facies distribution and stratal geometry of basins.

One of the most important process in basin evolution is the erosion and deposition mechanism of sediments. Authors usually distinguish between fluid flow and dynamic-slope models of the sedimentation erosion processes (see [R92], [R97]). The first ones use fluid flow equations and empirical algorithms to simulate the transport of sediments in the hydrodynamic flow field (see e.g. [TH89]). They provide an accurate description of depositional processes for small scales in time and space. At larger scale such as basin scales, fluid flow models are

[†]Institut Français du Pétrole, 1 et 4 av. de Bois Préau 92852 Rueil Malmaison Cedex
[‡]Département de Mathématiques, Université de Marne la Vallée, 5 boulevard Descartes, Champs sur Marne, F-77454, Marnes la vallée, Cedex 2.
[§]LATP, Université de Provence, 39 rue Frédéric Joliot Curie, 13453 Marseille cedex 13.

computationally too expensive and dynamic-slope approaches are usually preferred.

These latter models act at a more macroscopic scale and use mass conservation equations of sediments combined with diffusive transport laws that average over several processes (such as river transport, creep, slumps and small slides). They provide a good description of depositional processes for time scales larger than, say, 10^5 yr and basin space scales (see [AH89], [R92], [TS94], [R97], [G97], [GJD98],[GJ99]).

In multi-lithology approaches, sediments are modeled as a mixture of several lithologies characterized by different grain size populations. The set of equations accounts for the mass conservation of each lithology in the basin, knowing the surficial fluxes, a vertical compaction model (usually given by depth-porosity empirical laws for the lithologies), and an isostatic model for the lithosphere flexure (usually taken as a beam equation).

The main surficial transport process is a multi-lithology diffusion model introduced by [R92] for which fluxes are proportional to the slope of the topography as well as a lithology fraction defined at the surface of basin (see also [G97], [GJ99], [QAD00]). Diffusion coefficients are non-linear functions of the elevation (or equivalently the bathymetry) to model the transition from non-marine to marine diffusion that can differ from up to one or two order of magnitude.

However, it is well known that sedimentation and erosion are non symmetric processes. To be transported by surficial processes, as described by [AH89], material must first be produced in situ by weathering processes depending on climate, elevation, compaction of sediments, ... This production is modeled in [AH89] by a weathering rate also called soil production rate depending on the sediment depth with parameters function of climate. Then, on each cell of the discrete model, the sediment fluxes at the edges are constrained such that erosion cannot exceed the available soil thickness.

In [G97] or [GJ99], the model is slightly different in the sense that it directly prescribes a maximum erosion rate (defined as the partial time derivative of the sediment thickness) depending on climate, elevation, composition, and the age of the sediment.

As illustrated by [AH89], if the weathering rate is low, it can become the dominant process for erosion which is no longer governed by a diffusion transport while sedimentation is still diffusion transport limited.

It appears that the coupling of the weather limited model and the diffusion transport model is an essential issue for modeling depositional processes. Nevertheless, this question is not clearly addressed in [AH89] and is only referred to as "a diffusive transport with fluxes limited by available sediment" without a detailed description of the coupling between both processes. So far, we are not aware of any mathematical description of the coupling between weathering limited and diffusive transport models. The main objective of this paper is to propose such a mathematical model from which we are able to derive more efficient numerical algorithms for stratigraphic simulations.

A model taking into account the dissymmetry between erosion and sedimentation is also proposed in [R97]. The author uses a correction of the diffusion coefficient by a porosity ratio (sediment porosity over the depositional porosity) equal to one for sedimentation and lower than one for erosion. This ratio acts as a flux limitor, but, being independent on the fluxes (or the slope), it will fail to correctly freeze the erosion at the maximum soil production rate. Similarly a pointwise dependency of the diffusion coefficient on the erosion rate will also fail since, as we shall see in the subsequent development, the flux limitor satisfying the erosion rate constraint is actually a *global function* of the total flux.

Our approach starts from the numerical model developed at the discrete level in [G97]. In this model, the weather limited erosion is written as an inequality constraint on the partial time derivative of the sediment thickness (erosion or sedimentation rate). Then, the main idea is to threshold the edges output fluxes along the steepest descent paths in order to satisfy the maximal erosion rate constraint.

In this work, we propose an extension of this discrete model at the continuous level leading to a mathematical formulation coupling the multi-lithology diffusion transport equations to any weather limited model similar to the ones proposed by [AH89], [TS94] or [G97].

The basic idea of our mathematical formulation is first to impose the inequality constraint on the erosion rate and secondly to limit the fluxes by a factor λ constrained to be less than one (i.e. the fluxes are lower or equal to the diffusion fluxes). Then, the coupling between both models is obtained by imposing that the inequality constraints on the erosion rate and on the flux limitor, satisfy complementarity conditions. In other words, whenever the maximal erosion rate constraint is not active, then fluxes are equal to diffusion fluxes (active constraint $\lambda = 1$), and conversely, whenever the flux limitor is strictly lower than one (inactive constraint $\lambda < 1$), then the maximal erosion rate constraint is active.

It will be shown at the discrete level that the flux limitor λ, satisfying the above complementarity constraints, *maximizes* globally the fluxes such that the erosion rate cannot exceed the soil production rate whereas the fluxes cannot exceed the diffusion fluxes.

This formulation will allow us to design an efficient numerical algorithm for the simulation of the model using a finite volume discretization in space, a fully implicit time integration, and a Newton algorithm for the non-linear system adapted to complementarity constraints.

The remaining of the paper outlines as follows. In section 2, we introduce the mathematical model for the coupling of multi-lithology diffusive depositional processes with weather limited erosion models. In section 3, a finite volume discretization with implicit time integration is derived which is shown to be unconditionally stable. In section 4, we detail the Newton algorithm for the treatment of complementarity constraints. Section 5 is devoted to a 2D and a 3D basin simulation examples.

2 Mathematical model

A basin model specifies the geometry defined by the basin horizontal extension (of dimension two for 3D basin models and one for 2D basin models), the position of its base due to vertical tectonics displacements, and the sea level variations. It provides a description of the sediments (single lithology or multi-lithology models, porosity laws). Finally it specifies the sediment transport laws and their coupling, as well as the sediment fluxes at the boundary of the basin (boundary conditions). As they do not raise difficulties and for the sake of simplicity, we shall not consider in the sequel nor the tectonics displacements nor the compaction of the sediments.

The projection of the basin on a reference horizontal plane is considered as a fixed domain $\Omega \subset \mathbb{R}^d$ of boundary $\partial\Omega$, defining the horizontal extension of the basin, with $d = 1$ for two dimensional basin models and $d = 2$ for three dimensional models. We shall denote by z the vertical coordinate of a point in $\Omega \times \mathbb{R}$ with respect to the reference horizontal plane. For a given time $T > 0$, let $\mathcal{D}$ denote the domain $\Omega \times (0, T)$, and let $\mathbf{n}$ be the normal outward to $\partial\Omega$.

Let us denote by $h(x,t)$ the vertical coordinate of the surface of the basin at time $t \in (0,T)$ for all $x \in \Omega$, which parameterizes the topography of the basin. The variable h also represents the sediment thickness (positive or negative). Let $H_m(t)$ denote the vertical coordinate of the sea level at time t and

$$b(x,t) = h(x,t) - H_m(t)$$

the bathymetry at the surface of the basin for $(x,t) \in \mathcal{D}$.

In order to clarify the presentation, the model will be described in three steps:

1 the diffusion model where sediments consist of a single lithology.

2 the weather limited diffusion model for which a maximum erosion rate constraint is added to the previous model,

3 the full model for which sediments are in addition considered as a mixture of L lithologies.

2.1 Single lithology diffusion model

It is known from [AH89] that the evolution of the topography h in a sedimentary basin is well described by non linear parabolic equation solutions. Let $\psi(b)$ denote a strictly increasing function of the bathymeytry b, φ be the flux boundary condition at the boundary $\partial\Omega \times (0,T)$, and h^0 the initial topography at time $t = 0$ defined on Ω. The flux $\mathbf{f}$ of sediments at the surface of the basin (unit in m^2/yr) is given by the diffusion law

$$\mathbf{f} = -\nabla\psi. \tag{1}$$

The topography h satisfies the following non-linear parabolic equation accounting for the conservation of the sediment thickness.

Given $\varphi,\ h_0,\ H_m,\ \psi$, find h such that

$$\begin{aligned} \partial_t h - \operatorname{div}(\nabla\psi(b)) &= 0 && \text{on } \mathcal{D}, \\ -\nabla\psi(b)\cdot\mathbf{n} &= \varphi && \text{on } \partial\Omega \times (0,T), \\ h|_{t=0} &= h^0 && \text{on } \Omega. \end{aligned} \tag{2}$$

The non-linear dependence of ψ on the bathymetry b accounts for the fact that the diffusion coefficient $k(b) = \frac{d\psi}{db}(b)$ is usually of different orders of magnitude in marine ($b < 0$) and continental environnements ($b \geq 0$). Such a function is typically given by

$$\psi(b) = \begin{cases} k_m\, b & \text{if } b < 0, \\ k_c\, b & \text{otherwise} \end{cases}$$

where $k_c > 0$ (resp. $k_m > 0$) is the continental (resp. marine) diffusion coefficient parameter.

An example of a 2D basin ($d = 1$) is sketched in figure 1 with $\Omega = (0, L_b)$. The figure displays at time t the main variables of the model i.e. the sediment thickness or topography h, the sea level H_m, the bathymetry $b = h - H_m$, and the boundary flux φ (in this case an output flux $\varphi(L_b,t)$ at $x = L_b$ and an input flux $\varphi(0,t)$ at $x = 0$).

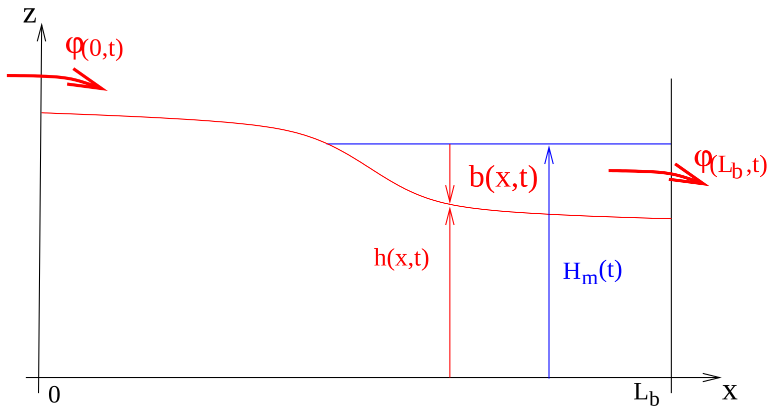

Figure 1: Example of a 2D sedimentary basin ($d = 1$) for the single-lithology model

2.2 Weather limited model

Diffusion models assume that sedimentation and erosion are symmetric processes since the diffusion coefficient $k(b)$ is independent on the sedimentation ($\partial_t h \geq 0$) or erosion ($\partial_t h < 0$) rate $\partial_t h$. Actually, as stated in [AH89], sediments must first be produced in situ by weathering processes prior to be transported by surficial erosion. This limitation is modeled in [G97] and [GJ99] through a maximum erosion rate $-E \leq 0$ (unit in m/yr) such that

$$\partial_t h \geq -E.$$

For the sake of simplicity, we shall assume in the sequel that E is a non negative constant although in more realistic models E depends on other variables such as the bathymetry b. The model is termed weather limited when the constraint $\partial_t h \geq -E$ is active i.e. $\partial_t h = -E$.

The coupling of the weather limited and diffusion models is clearly an essential issue since both diffusive sedimentation or erosion and weather limited erosion can clearly occur at the same time in a basin.

Nevertheless, this question has not been addressed rigorously so far. Although coupled single lithology numerical simulations are performed in [AH89] and [TS94], the coupling model is never made explicit. The main explanation is that the coupling has only been developed at the discrete level. This discrete coupling has been extended to multi-lithology models in [G97] and is detailed for a finite volume discretization in space and an explicit time integration scheme. The basic idea is to threshold the diffusion output fluxes at the edges of the finite volumes along the discrete steepest descent paths such that the limited fluxes are maximum, and the solution satisfies the maximum erosion rate constraint on each cell.

The derivation of the continuous model mimics the discrete scheme defined in [G97]. A new unknown λ is introduced, satisfying $\lambda \leq 1$ and playing the role of a flux limitor leading to the new definition of the flux

$$\mathbf{f} = -\lambda \, \nabla\psi(b)$$

and the new conservation equation of the sediment thickness h

$$\partial_t h - \mathrm{div}\Big(\lambda \, \nabla\psi(b)\Big) = 0 \text{ on } \mathcal{D}.$$

In order to close the model it is required that

(i) if the erosion rate constraint is inactive $\partial_t h > -E$ then $\lambda = 1$ i.e. the flux $\mathbf{f}$ is equal to the diffusion flux (1),

(ii) if $\lambda < 1$, then the constraint on the erosion rate is active i.e. $\partial_t h = -E$.

Such conditions are known as complementarity conditions for which we introduce the following notation: let $\mathcal{U}$ be any function from $\mathbb{R}^2$ to $\mathbb{R}$ such that

$$\mathcal{U}(A,B) = 0 \text{ iff } \begin{cases} A\,B = 0, \\ A \geq 0, \\ B \geq 0, \end{cases}$$

for $(A,B) \in \mathbb{R}^2$. As illustrated in figure 2, the complementarity conditions $\mathcal{U}(A,B) = 0$ equivalently mean that the point (A,B) is in the union of the two positive half axes.

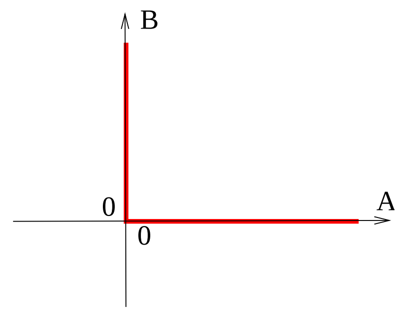

Figure 2: Unilateral conditions $\mathcal{U}(A,B) = 0$.

Then, the above closure conditions (i) and (ii) state that

$$\mathcal{U}\Big(\partial_t h + E, 1 - \lambda\Big) = 0 \text{ on } \mathcal{D}. \tag{3}$$

Let $\Sigma_- = \{(x,t) \in \partial\Omega \times (0,T), \varphi(x,t) < 0\}$ and $\Sigma_+ = \{(x,t) \in \partial\Omega \times (0,T), \varphi(x,t) \geq 0\}$. On the input boundary Σ_-, the boundary condition is unchanged. On the output boundary Σ_+ the boundary condition has to be adapted since the output flux φ may have to be limited to satisfy the maximum erosion rate constraint. This is again achieved by imposing the following complementarity conditions

$$\mathcal{U}\Big(\varphi - \mathbf{f}\cdot\mathbf{n}, \partial_t h + E\Big) = 0 \text{ on } \Sigma_+, \tag{4}$$

which lead to a switch from a flux boundary condition when $\partial_t h + E > 0$ to a Dirichlet boundary condition on the time derivative of h when $\mathbf{f}\cdot\mathbf{n} < \varphi$.

Below, we summarize the single-lithology model under maximum erosion rate constraint.

Given φ, h_0, H_m, ψ, E, find h, λ such that

$$\begin{aligned} \partial_t h - \operatorname{div}(\lambda \nabla \psi(b)) &= 0 && \text{on } \mathcal{D}, \\ \mathcal{U}(\partial_t h + E, 1 - \lambda) &= 0 && \text{on } \mathcal{D}, \\ -\lambda \nabla \psi(b)\cdot\mathbf{n} &= \varphi && \text{on } \Sigma_-, \\ \mathcal{U}(\partial_t h + E, \varphi + \lambda\nabla\psi(b)\cdot\mathbf{n}) &= 0 && \text{on } \Sigma_+, \\ h|_{t=0} &= h^0 && \text{on } \Omega. \end{aligned} \tag{5}$$

2.3 Extension to the multi-lithology model

In such models, the sediments are described as a mixture of L lithologies characterized by their grain size population. Each lithology, $i = 1, \cdots, L$, is considered as an uncompressible material of constant grain density and null porosity (no compaction).

In addition to the evolution of the topography h, the model describes the composition of the sediments at each point of the basin domain $\{(x, z),\ \text{such that } x \in \Omega,\ z < h(x,t)\}$ for all time $t \in (0, T)$.

The composition of the sediments inside the basin is modeled by their concentration $c_i(x, z, t)$ in the lithology i for all $i = 1, \cdots, L$, defined on the domain

$$\mathcal{B} = \{(x, z, t) \text{ such that } (x, t) \in \mathcal{D},\ z < h(x, t)\}.$$

and such that

$$c_i \geq 0 \text{ and } \sum_{i=1}^{L} c_i = 1 \text{ on } \mathcal{B}.$$

Since the compaction is not considered, there is no evolution in time of the concentrations c_i inside the basin such that for all $i = 1, \cdots, L$, the concentration c_i satisfies the conservation equation

$$\partial_t c_i = 0 \text{ on } \mathcal{B}.$$

The initial composition of the basin is given by the concentrations c_i^0 defined on the domain $\mathcal{B}^0 = \{(x, z),\ \text{such that } x \in \Omega,\ z < h^0(x)\}$, such that $c_i^0 \geq 0$ for all $i = 1, \cdots, L$, and $\sum_{i=1}^{L} c_i^0 = 1$.

The evolution of the concentration c_i is governed for each $i = 1, \cdots, L$ by an input boundary condition at the surface of the basin $z = h(x, t)$ in the case of sedimentation $\partial_t h > 0$. This input boundary condition is given by the new variable c_i^s called surface concentration defined on the domain $\mathcal{D}$ for each $i = 1, \cdots, L$ and such that

$$c_i^s \geq 0 \text{ and } \sum_{i=1}^{L} c_i^s = 1 \text{ on } \mathcal{D}.$$

All together this leads to the following first set of conservation equations for the multi-lithology model:

$$\left\{ \begin{aligned} \partial_t c_i &= 0 && \text{on } \mathcal{B}, \\ c_i|_{z=h} &= c_i^s && \text{on } \mathcal{D}_+, \\ c_i|_{t=0} &= c_i^0 && \text{on } \mathcal{B}^0, \end{aligned} \right. \tag{6}$$

with

$$\mathcal{D}_+ = \{(x, t) \in \mathcal{D} \text{ such that } \partial_t h(x, t) > 0\}.$$

In the case of sedimentation $\partial_t h > 0$, the surface concentrations $c_i^s, i = 1, \cdots, L$ define the composition of the sediments deposited at the top of the basin and reduce to $c_i^s(x, t) = c_i(x, h(x, t), t)$ for all $i = 1, \cdots, L$ and all (x, t) such that $\partial_t h(x, t) > 0$. However, in the erosive mode $\partial_t h \leq 0$, the surface concentrations are no longer connected to the concentrations c_i at the top of the basin. In that case, they represent the concentrations of the sediments passing through the surface as they appear in the following definition of the surficial fluxes.

In order to close the system, we need to extend the conservation equations (5) to the multi-lithology setting. This is achieved using the hillslope transport model introduced in

[R92]. Let ψ_i, $i = 1, \cdots, L$ be strictly increasing functions of the bathymetry b, then for each $i = 1, \cdots, L$,

$$\mathbf{f}_i = -c_i^s \lambda \nabla \psi_i(b)$$

defines the surficial flux of the sediments in lithology i, proportional to the gradient of ψ_i and to the surface concentration c_i^s, and limited by the flux limitor λ. We denote by $k_i(b) = \frac{d\psi_i}{db}(b)$ the diffusion coefficient of the lithology i. Then, the set of equations accounts, for each lithology $i = 1, \cdots, L$, for the conservation of the sediment thickness in lithology i defined for all $(x,t) \in \mathcal{D}$ as

$$h_i(x,t) = \int_0^{h(x,t)} c_i(x,z,t)dz,$$

with $\sum_{i=1}^L h_i = h$ on $\mathcal{D}$. It states that

$$\begin{cases} \partial_t h_i + \mathrm{div}\mathbf{f}_i = 0 & \text{on } \mathcal{D} \text{ for } i = 1, \cdots, L, \\ \sum_{i=1}^L c_i^s = 1 & \text{on } \mathcal{D}, \end{cases} \tag{7}$$

together with the complementarity conditions (3). The initial condition is still defined by $h|_{t=0} = h^0$. The boundary condition on the output boundary Σ_+ is also given by (4) with the total flux $\mathbf{f} = \sum_{i=1}^L \mathbf{f}_i$. The input boundary conditions are adapted by prescribing the input fluxes $\mathbf{f}_i \cdot \mathbf{n} = \bar{\mu}_i \varphi$ on Σ_- for all $i = 1, \cdots, L$ where $\bar{\mu}_i, i = 1, \cdots, L$ are given functions defined on Σ_- such that $\bar{\mu}_i \geq 0$ and $\sum_{i=1}^L \bar{\mu}_i = 1$.

The 2D basin example is completed in figure 3 to include in addition to the previous variables, the sediment concentrations c_i, the surface sediment concentrations c_i^s, and the boundary fluxes (in this case an output flux $\varphi(L_b, t)$ at $x = L_b$ and input fluxes $\bar{\mu}_i(0,t)\varphi(0,t)$ for each lithology at $x = 0$).

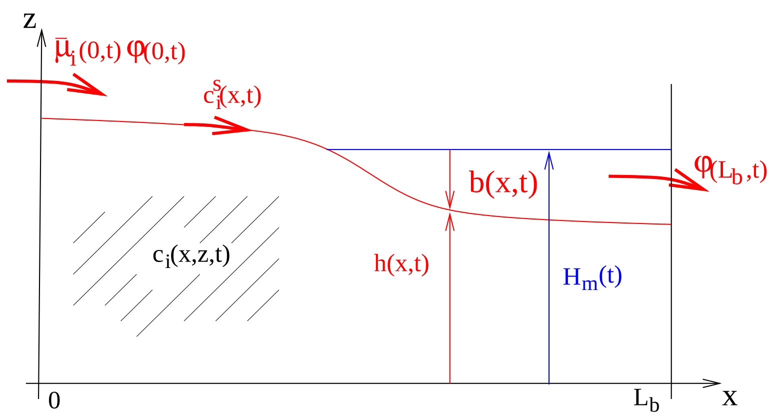

Figure 3: Example of a 2D sedimentary basin ($d = 1$) for the multi-lithology model

In summary, here is the multi-lithology model under maximum erosion rate constraint.

Given

$$\varphi,\ h_0,\ H_m,\ E,\ c_i^0,\ \bar{\mu}_i,\ \psi_i \text{ for all } i = 1,\cdots,L$$

Find

$$h,\ \lambda,\ c_i,\ c_i^s \text{ for all } i = 1,\cdots,L$$

such that

$$\begin{array}{rcll}
\multicolumn{4}{l}{\text{Conservation equations on } \mathcal{D}}\\
\partial_t h_i - \operatorname{div}(c_i^s \lambda \nabla \psi_i(b)) &=& 0 & \text{on } \mathcal{D},\\
\sum_{i=1}^L c_i^s &=& 1 & \text{on } \mathcal{D},\\
\mathcal{U}(\partial_t h + E, 1-\lambda) &=& 0 & \text{on } \mathcal{D},\\
-c_i^s \lambda \nabla \psi_i(b)\cdot \mathbf{n} &=& \bar{\mu}_i \varphi & \text{on } \Sigma_-,\\
\mathcal{U}(\partial_t h + E, \varphi + \sum_{i=1}^L c_i^s \lambda \nabla \psi_i(b)\cdot \mathbf{n}) &=& 0 & \text{on } \Sigma_+,\\
h|_{t=0} &=& h^0 & \text{on } \Omega,\\
\multicolumn{4}{l}{\text{Conservation equations on } \mathcal{B}}\\
\partial_t c_i &=& 0 & \text{on } \mathcal{B},\\
c_i|_{z=h} &=& c_i^s & \text{on } \mathcal{D}_+,\\
c_i|_{t=0} &=& c_i^0 & \text{on } \mathcal{B}^0.
\end{array} \qquad (8)$$

One of the main advantage of this formulation is to allow the definition of an efficient numerical scheme using a fully implicit time integration and a Newton algorithm suited to complementarity constraints. This is the purpose of the next two sections.

3 Finite Volumes Discretization

3.1 The discrete scheme

The system (8) is discretized by a fully implicit time integration and a finite volume method with cell centered variables.

For the sake of simplicity, let us consider a rectangular domain Ω endowed with a Cartesian mesh $\mathcal{K}$ (non structured meshes could be considered as well). Let $|\kappa|$ denote the d dimensional volume of the cell $\kappa \in \mathcal{K}$, and $d(\kappa,\kappa')$ be the distance between the centers of the cells κ and κ' of $\mathcal{K}$. Let Σ_κ denote the set of the edges of the cell κ, and $|\sigma|$ be the $d-1$ dimensional measure (set to 1 for $d=1$) of an edge $\sigma \in \Sigma_\kappa$.

The time discretization is denoted by $t^n, n \in \mathbb{N}$ such that $t^0 = 0$, and $\Delta t^{n+1} := t^{n+1} - t^n > 0$. In the following, the superscript n, $n \in \mathbb{N}$, will be used to denote that the variables are considered at time t^n.

Let us now introduce the primary variables of the discrete problem (see figures 4 and 5). For all $\kappa \in \mathcal{K}$, and $n \in \mathbb{N}$, we denote by h_κ^{n+1} (resp. λ_κ^{n+1}, and $c_{i,\kappa}^{s,n+1}$ for $i = 1,\cdots,L$) the approximation at time t^{n+1} and in the cell κ of the sediment thickness h (resp. of the flux limitor λ, and of the surface concentrations c_i^s for $i = 1,\cdots,L$). For all $\kappa \in \mathcal{K}$, $n \in \mathbb{N}$, and $i = 1,\cdots,L$, $c_{i,\kappa}^{n+1}$ is a function defined on $(-\infty, h_\kappa^{n+1})$, which approximates at time t^{n+1} and in the cell κ the concentration $c_{i,\kappa}$.

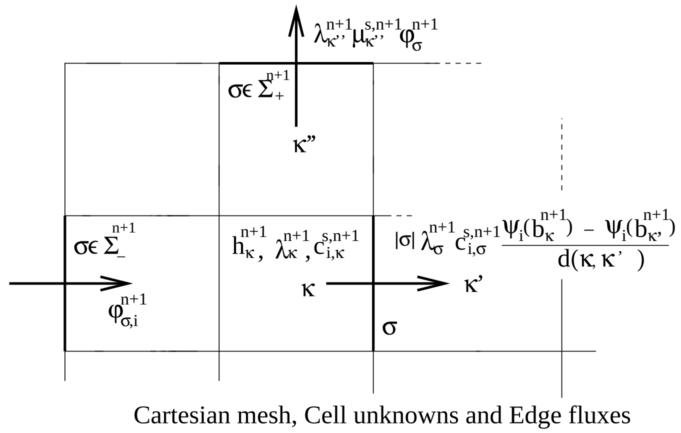

Figure 4: Cartesian mesh $\mathcal{K}$, cell unknowns $(h_\kappa^{n+1}, \lambda_\kappa^{n+1}, c_{i,\kappa}^{s,n+1})$, and approximations of the fluxes at the edge $\sigma \in \Sigma_k \cap \Sigma_{k'}$ between two cells κ and κ', at an input edge $\sigma \in \Sigma_-^{n+1}$, and at an output edge $\sigma \in \Sigma_+^{n+1} \cap \Sigma_{k''}$.

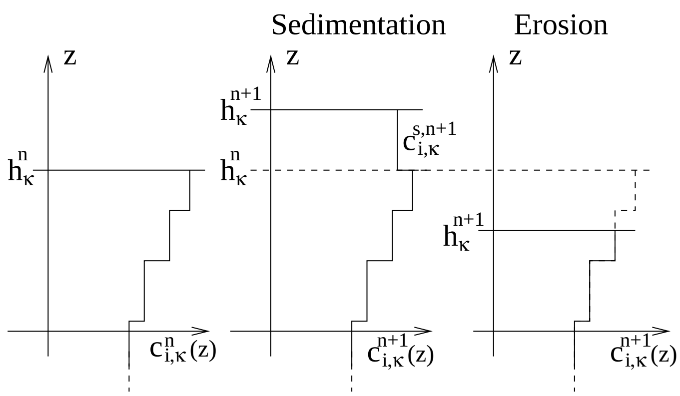

Figure 5: Concentration $c_{i,\kappa}^n$ at time t^n and update at time t^{n+1} of the concentration $c_{i,\kappa}^{n+1}$ in the sedimentation or erosion cases.

We suppose that, for all control volume $\kappa \in \mathcal{K}$, the following initial values are defined:

1. h_κ^0 is an approximation of h^0 in the cell κ,
2. $c_{i,\kappa}^0$, for all species i, is a piecewise constant non negative approximation of c_i^0 in the cell κ defined on $(-\infty, h_\kappa^0)$ and such that $\sum_{i=1}^L c_{i,\kappa}^0 = 1$.

The discretization of the conservation equations (7) is obtained by integration over the cell κ and between the times t^n and t^{n+1}

$$\int_{t^n}^{t^{n+1}} \int_\kappa \partial_t h_i \, dx \, dt + \sum_{\sigma \in \Sigma_\kappa} \int_{t^n}^{t^{n+1}} \int_\sigma -\lambda \, c_i^s \, \nabla \psi_i(b) \cdot \mathbf{n}_\kappa \, d\sigma \, dt = 0,$$

where $\mathbf{n}_\kappa$ is the normal to σ outward to κ, followed by approximations of the accumulation and flux terms detailed below.

As illustrated in figure 4, the flux

$$\frac{1}{\Delta t^{n+1}} \int_{t^n}^{t^{n+1}} \int_\sigma -\lambda \, c_i^s \, \nabla \psi_i(b) \cdot \mathbf{n}_\kappa \, d\sigma \, dt \tag{9}$$

at the edge $\sigma \in \Sigma_\kappa \cap \Sigma_{\kappa'}$ between the cells κ and κ' is approximated by

$$|\sigma| \lambda_\sigma^{n+1} c_{i,\sigma}^{s,n+1} \frac{\psi_i(b_\kappa^{n+1}) - \psi_i(b_{\kappa'}^{n+1})}{d(\kappa,\kappa')},$$

where $b_\kappa^{n+1} = h_\kappa^{n+1} - H_m(t^{n+1})$ is the bathymetry in the cell κ at time t^{n+1},

$$\lambda_\sigma^{n+1} = \begin{cases} \lambda_\kappa^{n+1} \text{ if } b_\kappa^{n+1} > b_{\kappa'}^{n+1}, \\ \lambda_{\kappa'}^{n+1} \text{ otherwise }, \end{cases}$$

and

$$c_{i,\sigma}^{s,n+1} = \begin{cases} c_{i,\kappa}^{s,n+1} \text{ if } b_\kappa^{n+1} > b_{\kappa'}^{n+1}, \\ c_{i,\kappa'}^{s,n+1} \text{ otherwise }. \end{cases}$$

This approximation is implicit in time and uses an upstream weighted evaluation of λ and c_i^s at the edge σ between the cells κ and κ', and a two point approximation of the gradient of ψ_i in the normal direction. These choices are the key ingredients to obtain the stability of the numerical scheme discussed in the next section.

To define the approximation of the flux (9) for edges σ at the boundary $\partial\Omega$, let us introduce the subset Σ_-^{n+1} (resp. Σ_+^{n+1}) of $\bigcup_{\kappa\in\mathcal{K}} \Sigma_\kappa$ such that Closure$\{x,\ (x,t^{n+1}) \in \Sigma_-\} = \bigcup_{\sigma\in\Sigma_-^{n+1}} \bar{\sigma}$ (resp. Closure$\{x,\ (x,t^{n+1}) \in \Sigma_+\} = \bigcup_{\sigma\in\Sigma_+^{n+1}} \bar{\sigma}$).

Then, for all $\sigma \in \Sigma_-^{n+1} \cap \Sigma_\kappa$, the flux (9) is given by the approximation

$$\varphi_{\sigma,i}^{n+1} = \int_\sigma \bar{\mu}_i(x,t^{n+1})\, \varphi(x,t^{n+1})\, d\sigma$$

of the input boundary condition.

Let $\mu_{i,\kappa}^{s,n+1}$ denote the fractional flow $\frac{c_{i,\kappa}^{s,n+1} k_i(b_\kappa^{n+1})}{\sum_{j=1}^L c_{j,\kappa}^{s,n+1} k_j(b_\kappa^{n+1})}$. On the output boundary, for all $\sigma \in \Sigma_+^{n+1} \cap \Sigma_\kappa$, the flux (9) is approximated by

$$\lambda_\kappa^{n+1} \mu_{i,\kappa}^{s,n+1} \varphi_\sigma^{n+1} \text{ with } \varphi_\sigma^{n+1} = \int_\sigma \varphi(x,t^{n+1})\, d\sigma.$$

The approximation $|\kappa|\Delta h_{i,\kappa}^{n+1}$ of the accumulation term

$$\int_{t^n}^{t^{n+1}} \int_\kappa \partial_t h_i(x,t)\, dx\, dt = \int_\kappa \Big(\int_0^{h(x,t^{n+1})} c_i(x,z,t^{n+1})\, dz - \int_0^{h(x,t^n)} c_i(x,z,t^n)\, dz \Big) dx$$

is defined by

$$|\kappa|\Delta h_{i,\kappa}^{n+1} = |\kappa| \Big(\int_0^{h_\kappa^{n+1}} c_{i,\kappa}^{n+1}(z)\, dz - \int_0^{h_\kappa^n} c_{i,\kappa}^n(z)\, dz \Big). \tag{10}$$

The approximate concentration $c_{i,\kappa}^{n+1}$ is the solution at time t^{n+1} of the conservation equation

$$\begin{cases} \partial_t c_{i,\kappa}(z,t) = 0, & \text{for all } t^n < t < t^{n+1}, z < h_\kappa^n + (t-t^n)\frac{h_\kappa^{n+1}-h_\kappa^n}{\Delta t^{n+1}}, \\ c_{i,\kappa}(h_\kappa(t),t)) = c_{i,\kappa}^{s,n+1} & \text{if } h_\kappa^{n+1} > h_\kappa^n, \\ c_{i,\kappa}(z,t^n) = c_{i,\kappa}^n(z) & \text{for all } z < h_\kappa^n. \end{cases} \tag{11}$$

The integration of this equation is straightforward considering separately the sedimentation ($h_\kappa^{n+1} > h_\kappa^n$) and erosion ($h_\kappa^{n+1} \le h_\kappa^n$) cases. It leads to the update formulae (14) and (15) illustrated in figure 5. We also deduce the new expression of the accumulation term $\Delta h_{i,\kappa}^{n+1}$ given in (14) and (15).

The discretization of the complementarity constraints (3) is defined by

$$\mathcal{U}\Big(h_\kappa^{n+1} - \mathcal{H}_\kappa^{n+1}, 1 - \lambda_\kappa^{n+1}\Big) = 0,$$

where $\mathcal{H}_\kappa^{n+1}$ is the solution $h_\kappa^n - E\Delta t^{n+1}$ at time t^{n+1} to the erosion rate constraint equation between t^{n+1} and t^n: $\partial_t \mathcal{H}_\kappa(t) = -E$, $\mathcal{H}_\kappa(t^n) = h_\kappa^n$.

Finally, the discrete problem summarizes as follows.

Given H_m, $\psi_i(b)$, h_κ^0, and $c_{i,\kappa}^0$ for all $\kappa \in \mathcal{K}$, $i = 1, \cdots, L$, φ_σ^{n+1} for all $n \geq 0$, $\sigma \in \Sigma_+^{n+1}$, and $\varphi_{\sigma,i}^{n+1}$ for all $i = 1, \cdots, L$, $n \geq 0$, $\sigma \in \Sigma_-^{n+1}$,

Find h_κ^{n+1}, λ_κ^{n+1}, and $c_{i,\kappa}^{s,n+1}$, $c_{i,\kappa}^{n+1}$ for all $\kappa \in \mathcal{K}$, $n \geq 0$, $i = 1, \cdots, L$ such that for all $k \in \mathcal{K}$ and $i = 1, \cdots, L$:

Conservation of surface sediments:

$$\begin{aligned}\frac{\Delta h_{i,\kappa}^{n+1}}{\Delta t^{n+1}}|\kappa| + &\sum_{\sigma \in \Sigma_\kappa \cap \Sigma_{\kappa'}} \lambda_\sigma^{n+1} c_{i,\sigma}^{s,n+1} |\sigma| \frac{\psi_i(b_\kappa^{n+1}) - \psi_i(b_{\kappa'}^{n+1})}{d(\kappa,\kappa')} + \\ &\sum_{\sigma \in \Sigma_\kappa \cap \Sigma_-^{n+1}} \varphi_{\sigma,i}^{n+1} + \lambda_\kappa^{n+1} \mu_{i,\kappa}^{s,n+1} \sum_{\sigma \in \Sigma_\kappa \cap \Sigma_+^{n+1}} \varphi_\sigma^{n+1} = 0\end{aligned} \tag{12}$$

$$\sum_{i=1}^{L} c_{i,\kappa}^{s,n+1} = 1, \tag{13}$$

Conservation of column sediments:

$$\text{if } h_\kappa^{n+1} \geq h_\kappa^n \text{ (sedimentation)} \quad \begin{cases} \Delta h_{i,\kappa}^{n+1} = c_{i,\kappa}^{s,n+1}(h_\kappa^{n+1} - h_\kappa^n) \\ c_{i,\kappa}^{n+1}(z) = c_{i,\kappa}^n(z) \text{ for all } z < h_\kappa^n \\ c_{i,\kappa}^{n+1}(z) = c_{i,\kappa}^{s,n+1} \text{ for all } z \in (h_\kappa^n, h_\kappa^{n+1}) \end{cases} \tag{14}$$

$$\text{else (erosion)} \quad \begin{cases} \Delta h_{i,\kappa}^{n+1} = \int_{h_\kappa^n}^{h_\kappa^{n+1}} c_{i,\kappa}^n(z)dz \\ c_{i,\kappa}^{n+1}(z) = c_{i,\kappa}^n(z) \text{ for all } z < h_\kappa^{n+1} \end{cases} \tag{15}$$

Constraints:

$$\mathcal{U}\Big(h_\kappa^{n+1} - \mathcal{H}_\kappa^{n+1}, 1 - \lambda_\kappa^{n+1}\Big) = 0, \tag{16}$$

Let us note that at each time step from t^n to t^{n+1}, the computation of the unknowns h_κ^{n+1}, λ_κ^{n+1}, and $c_{i,\kappa}^{s,n+1}$ decouples from the update of the column sediment concentrations $c_{i,\kappa}^{n+1}$.

3.2 Stability properties of the finite volumes discretization

An essential topic is the study of the non-negativity of the limitors and of the concentrations solutions to (12)-(16). It is possible to state such a result with a slight modification of the definition of the output boundary fluxes.

Proposition 3.1. *Let us assume for all time $t^{n+1}, n \geq 0$, the new definition $\mu_{i,\kappa}^{s,n+1} = c_{i,\kappa}^{s,n+1}$ for all $\kappa \in \mathcal{K}$ or alternatively $\varphi_\sigma^{n+1} = 0$ for all $\sigma \in \Sigma_+^{n+1}$.*

Then, any solution of the scheme (12)-(16) satisfies $\lambda_\kappa^{n+1} \in [0,1]$ and $c_{i,\kappa}^{s,n+1} \in [0,1]$ for all $i = 1, \ldots, L$, $n \geq 0$, $\kappa \in \mathcal{K}$, except for the degenerate points (κ, n).

The degenerate points (κ, n) are the points for which all the fluxes at the edges of the control volume κ vanish, and $h_\kappa^{n+1} = h_\kappa^n$. In that cases, the concentrations $c_{i,\kappa}^{s,n+1}$, $i = 1, \cdots, L$ can be arbitrarily chosen such that their sum over the species is equal to 1, and the flux limitor λ_κ^{n+1} is either arbitrary in the interval $(-\infty, 1]$ for $E = 0$ or equal to 1 for $E > 0$.

Proof: The proof is done by induction over n and over the control volumes $\kappa \in \mathcal{K}$ in decreasing topographical order.

For the highest topographical point(s) κ, the fluxes at the edges $\sigma \in \Sigma_\kappa$ are either output fluxes or input boundary fluxes $\varphi_{\sigma,i}^{n+1}$, $\sigma \in \Sigma_\kappa \cap \Sigma_-^{n+1}$, and therefore for all species i

$$\sum_{\sigma \in \Sigma_\kappa \cap \Sigma_{\kappa'},\, b_\kappa^{n+1} < b_{\kappa'}^{n+1}} \lambda_\sigma^{n+1} c_{i,\sigma}^{s,n+1} \, |\sigma| \frac{\psi_i(b_\kappa^{n+1}) - \psi_i(b_{\kappa'}^{n+1})}{d(\kappa, \kappa')} \leq 0. \tag{17}$$

Let us consider a control volume $\kappa \in \mathcal{K}$ and assume that the proposition holds for all the lower cells at time t^{n+1} and all the previous times $t^{l+1}, 0 \leq l < n$. It results from this induction hypothesis and the upwinding of λ and c_i^s that the inequality (17) also holds for all $i = 1, \cdots, L$.

Hence, the proof will be obtained if the proposition is proved at time t^{n+1}, assuming that the sediment concentrations $c_{i,\kappa}^n(z)$, $\kappa \in \mathcal{K}$, $z < h_\kappa^n$ are positive (which holds for $n = 0$) and that the inequality (17) holds.

Let us proceed by assuming that $h_\kappa^{n+1} - h_\kappa^n \leq 0$ (erosion). It results from the induction hypothesis over n and over the control volumes that

$$\lambda_\kappa^{n+1} c_{i,\kappa}^{s,n+1} \Big(\sum_{\sigma \in \Sigma_\kappa \cap \Sigma_{\kappa'},\, b_\kappa^{n+1} \geq b_{\kappa'}^{n+1}} |\sigma| \frac{\psi_i(b_\kappa^{n+1}) - \psi_i(b_{\kappa'}^{n+1})}{d(\kappa, \kappa')} + \sum_{\sigma \in \Sigma_\kappa \cap \Sigma_+^{n+1}} \varphi_\sigma^{n+1} \Big) \geq 0, \tag{18}$$

for all species i. In equation (18), either the term inside the brackets is strictly positive for all $i = 1, \cdots, L$ or it vanishes for all $i = 1, \cdots, L$. In the first case, it results from (13) that λ_κ^{n+1} and $c_{i,\kappa}^{s,n+1}$, $i = 1, \cdots, L$ are non negative. In the second case, the point (κ, n) is a degenerate point for which the concentrations $c_{i,\kappa}^{s,n+1}$, $i = 1, \cdots, L$ can be arbitrarily chosen such that $\sum_{i=1}^L c_{i,\kappa}^{s,n+1} = 1$. The flux limitor λ_κ^{n+1} can be also arbitrarily chosen in the interval $(-\infty, 1]$ if $E = 0$ but is equal to 1 from equations (16) if $E > 0$.

Let us now consider the sedimentation case for which $h_\kappa^{n+1} - h_\kappa^n > 0$. It results from (16) that $\lambda_\kappa^{n+1} = 1$. From equation (12) and the induction hypothesis we obtain that

$$c_{i,\kappa}^{s,n+1} \Big(\frac{h_\kappa^{n+1} - h_\kappa^n}{\Delta t^{n+1}} \, |\kappa| + \sum_{\sigma \in \Sigma_\kappa \cap \Sigma_{\kappa'},\, b_\kappa^{n+1} \geq b_{\kappa'}^{n+1}} |\sigma| \frac{\psi_i(b_\kappa^{n+1}) - \psi_i(b_{\kappa'}^{n+1})}{d(\kappa, \kappa')} + \sum_{\sigma \in \Sigma_\kappa \cap \Sigma_+^{n+1}} \varphi_\sigma^{n+1} \Big) \geq 0,$$

and hence $c_{i,\kappa}^{s,n+1} \geq 0$, for all $i = 1, \cdots, L$. □

As a consequence of the non negativity of λ_κ^{n+1} and of $c_{i,\kappa}^{s,n+1} \in [0,1]$, $n \geq 0$, $\kappa \in \mathcal{K}$, it is possible to deduce that the sediment thickness satisfies a discrete maximum principle (see

[EGH00] for examples of such proofs).

The next proposition provides a characterization of the limitors as the coefficients maximizing the edges total output fluxes (for given concentrations and sediment thicknesses) under the constraints $1-\lambda_\kappa^{n+1} \geq 0$ and $h_\kappa^{n+1} \geq \mathcal{H}_\kappa^{n+1}$. The proof is straightforward considering the cell conservation equations and complementarity constraints in decreasing topographical order.

Proposition 3.2. *Let κ_l, $l = 1, \cdots, \#\mathcal{K}$ be a decreasing topographical ordering of the cells (with $\#\mathcal{K}$ denoting the cardinality of the set $\mathcal{K}$). The limitors $\lambda_\kappa^{n+1}, k \in \mathcal{K}$ are given by $\lambda_{\kappa_l}^{n+1} = \min\Big(1, \frac{\alpha_{\kappa_l}}{\beta_{\kappa_l}}\Big)$ for $l = 1, \cdots, \#\mathcal{K}$, with*

$$\alpha_{\kappa_l} = E|\kappa_l| - \sum\nolimits_{i=1}^{L}\Big(\sum_{\sigma\in\Sigma_{\kappa_l}\cap\Sigma_{\kappa'},\, b_{\kappa_l}^{n+1}<b_{\kappa'}^{n+1}} \lambda_\sigma^{n+1} c_{i,\sigma}^{s,n+1}\, |\sigma| \frac{\psi_i(b_{\kappa_l}^{n+1}) - \psi_i(b_{\kappa'}^{n+1})}{d(\kappa_l,\kappa')} + \sum_{\sigma\in\Sigma_{\kappa_l}\cap\Sigma_-^{n+1}} \varphi_{\sigma,i}^{n+1}\Big),$$

$$\beta_{\kappa_l} = \sum\nolimits_{i=1}^{L} \sum_{\sigma\in\Sigma_{\kappa_l}\cap\Sigma_{\kappa'},\, b_{\kappa_l}^{n+1}\geq b_{\kappa'}^{n+1}} c_{i,\sigma}^{s,n+1}\, |\sigma| \frac{\psi_i(b_{\kappa_l}^{n+1}) - \psi_i(b_{\kappa'}^{n+1})}{d(\kappa_l,\kappa')} + \sum_{\sigma\in\Sigma_{\kappa_l}\cap\Sigma_+^{n+1}} \varphi_\sigma^{n+1}.$$

Note that for degenerate points (κ, n), λ_κ^{n+1} is set to 1. This formula also characterizes the unique solution of the following optimization problem: given the concentrations $c_{i,\kappa}^{s,n+1}, i = 1, \cdots, L$ and the sediment thicknesses h_κ^{n+1}, $\kappa \in \mathcal{K}$, find $\lambda^{n+1} = (\lambda_\kappa^{n+1})_{\kappa\in\mathcal{K}}$ maximum, in the sense of the vectorial ordering $\lambda' \geq \lambda$ iff $\lambda'_\kappa \geq \lambda_\kappa$ for all $\kappa \in \mathcal{K}$, and under the inequality constraints

$$\left\{\begin{array}{l} 1-\lambda_\kappa^{n+1} \geq 0,\ \kappa\in\mathcal{K},\\ \sum\nolimits_{i=1}^{L}\Big(\sum\limits_{\sigma\in\Sigma_\kappa\cap\Sigma_{\kappa'}} \lambda_\sigma^{n+1} c_{i,\sigma}^{s,n+1}\, |\sigma| \dfrac{\psi_i(b_\kappa^{n+1}) - \psi_i(b_{\kappa'}^{n+1})}{d(\kappa,\kappa')} \ + \sum\limits_{\sigma\in\Sigma_\kappa\cap\Sigma_-^{n+1}} \varphi_{\sigma,i}^{n+1}\Big) \ + \\ \qquad \lambda_\kappa^{n+1} \sum\limits_{\sigma\in\Sigma_\kappa\cap\Sigma_+^{n+1}} \varphi_\sigma^{n+1} \ \leq\ E|\kappa|,\ \kappa\in\mathcal{K}. \end{array}\right.$$

Remark 3.1. *From Proposition 3.2, the limitor λ exhibits a non local dependence on the edges total fluxes, which shows that a proper coupling of the weather limited and diffusion models could not be obtained with a limitor locally depending on the erosion rate.*

4 Non-linear solver

The non-linear system (12)-(16) is solved using a Newton algorithm adapted to complementarity constraints (see [EGH00]).

A binary phase index $\mathcal{I} = (\mathcal{I}_\kappa)_{\kappa\in\mathcal{K}} \in \{0,1\}^{\mathcal{K}}$ is introduced where $\mathcal{I}_\kappa = 1$ corresponds to the diffusion transport $\lambda_\kappa^{n+1} = 1$, $h_\kappa^{n+1} \geq \mathcal{H}_\kappa^{n+1}$, and $\mathcal{I}_\kappa = 0$ corresponds to the weather limited transport $h_\kappa^{n+1} = \mathcal{H}_\kappa^{n+1}$, $\lambda_\kappa^{n+1} \leq 1$.

For a fixed index phase $\mathcal{I}$, we define the variable y^{n+1} such that for all $k \in \mathcal{K}$

$$y_\kappa^{n+1} = \left\{\begin{array}{l} h_\kappa^{n+1} \text{ if } \mathcal{I}_\kappa = 1,\\ \lambda_\kappa^{n+1} \text{ if } \mathcal{I}_\kappa = 0.\end{array}\right.$$

Then, we denote by $\mathcal{R}^{n+1} : \mathbb{R}^{\mathcal{K}} \times (\mathbb{R}^{\mathcal{K}})^L \rightarrow (\mathbb{R}^{\mathcal{K}})^L \times \mathbb{R}^{\mathcal{K}}$, the residual of equations (12)-(13) as function of (y^{n+1}, c^{n+1}) for a fixed phase index $\mathcal{I}$, where c^{n+1} stands for the vector

$c_{i,\kappa}^{s,n+1}, \kappa \in \mathcal{K}, i = 1, \cdots, L.$

The Newton phase index algorithm performs a sequence of Newton iterations applied to the non-linear function $\mathcal{R}^{n+1}$ followed by updates of the phase index in order to satisfy the inequality constraints $\left(h_\kappa^{n+1} - \mathcal{H}_\kappa^{n+1}\right) \geq 0$ and $\left(1 - \lambda_\kappa^{n+1}\right) \geq 0$ for all $\kappa \in \mathcal{K}$.

If the solution satisfies at convergence $\lambda_\kappa^{n+1} \geq 0$ and $c_{i,\kappa}^{s,n+1} \geq 0$, for all $\kappa \in \mathcal{K}$, $i = 1, \cdots, L$, as proved in proposition 3.1, this is no longer the case of the Newton iterates. Hence, these constraints are also imposed during the update step by projections.

$$\text{Initialization: } \begin{cases} \mathcal{I}_\kappa^{n+1,0} = 1,\ y_\kappa^{n+1,0} = h_\kappa^n,\ \kappa \in \mathcal{K}, \\ c^{n+1,0} = c^n. \end{cases}$$

Solve for $q = 0, \cdots,$ until convergence

$$\begin{cases} \partial_{(y^{n+1},c^{n+1})} \mathcal{R}^{n+1}(y^{n+1,q}, c^{n+1,q})(\delta y, \delta c)^T = -\mathcal{R}^{n+1}(y^{n+1,q}, c^{n+1,q}), \\ (y^{n+1,q+1}, c^{n+1,q+1})^T = (y^{n+1,q}, c^{n+1,q})^T + (\delta y, \delta c)^T \end{cases}$$

$$\text{if } \mathcal{I}_\kappa^{n+1,q} = 1 \begin{cases} \text{if } h_\kappa^{n+1,q+1} - \mathcal{H}_\kappa^{n+1} < 0 \text{ then } \begin{cases} \mathcal{I}_\kappa^{n+1,q+1} = 0, \\ h_\kappa^{n+1,q+1} = \mathcal{H}_\kappa^{n+1} \end{cases} \\ \text{else } \mathcal{I}_\kappa^{n+1,q+1} = \mathcal{I}_\kappa^{n+1,q} \end{cases}$$

$$\text{if } \mathcal{I}_\kappa^{n+1,q} = 0 \begin{cases} \text{if } \lambda_\kappa^{n+1,q+1} > 1 \text{ then } \mathcal{I}_\kappa^{n+1,q+1} = 1 \text{ and } \lambda_\kappa^{n+1,q+1} = 1, \\ \text{else } \mathcal{I}_\kappa^{n+1,q+1} = \mathcal{I}_\kappa^{n+1,q},\ \lambda_\kappa^{n+1,q+1} := \max(0, \lambda_\kappa^{n+1,q+1}). \end{cases}$$

$$\left(c_{i,\kappa}^{s,n+1,q+1}\right)_{i=1}^{L} := \operatorname{Proj}_{\{d \in [0,1]^L, \sum_{i=1}^L d_i = 1\}} \left(c_{i,\kappa}^{s,n+1,q+1}\right)_{i=1,\cdots,L}$$

End

The Jacobian $\partial_{(y^{n+1},c^{n+1})} \mathcal{R}^{n+1}$ is clearly singular in the two following cases corresponding to non physical situations. Although these are excluded at convergence, they can occur during the Newton iterations.

The first case arises when, for a given cell κ, the erosion rate constraint is active $\mathcal{I}_\kappa^{n+1,q} = 0$ and all the fluxes at the edges $\sigma \in \Sigma_\kappa$ are input fluxes. Then, it results from the upwinding of λ that the column $\partial_{y_\kappa^{n+1}} \mathcal{R}^{n+1}$ of the Jacobian vanishes.

Similarly, when for a given cell κ, $h_\kappa^{n+1,q} - h_\kappa^n \leq 0$ (eroded cell) and all the fluxes at the edges $\sigma \in \Sigma_\kappa$ are input fluxes, then due to the upwinding of the surface sediment concentrations, the columns $\partial_{c_{i,k}^{s,n+1}} \mathcal{R}^{n+1}$, $i = 1, \cdots, L$, of the Jacobian contain only zero entries.

In such cases, we modify the Jacobian to avoid its singularity. Precisely, if $\sum_{i=1}^L \partial_{y_\kappa^{n+1}} \mathcal{R}_{i,\kappa}^{n+1} = 0$, then we set $\partial_{y_\kappa^{n+1}} \mathcal{R}_{1,\kappa}^{n+1} = \epsilon > 0$. In practice, it is more efficient to combine this strategy with a modification of the index phase and the Newton iterate during the update step which eliminates partially these non physical degenerate cases.

Similarly for $L > 1$, if $\partial_{c_{1,k}^{s,n+1}} \mathcal{R}_{1,\kappa}^{n+1} = 0$, then we set $\partial_{c_{i,k}^{s,n+1}} \mathcal{R}_{i,\kappa}^{n+1} = 1$ for $i = 1, \cdots, L$ and leave the concentrations $c_{i,k}^{s,n+1}$, $i = 1, \cdots, L$ unchanged at this Newton iteration.

4.1 Numerical examples

4.2 Delta Progradation

We consider the interval domain $\Omega = (0, L_b)$ with $L_b = 200$ km. The initial topography is given by the function $h^0(x) = 25e^{-8\frac{x}{L_b}} + 10$ m, and the eustatic sea level variations by

$H_m(t) = 25 + 5\cos(6t)$ m.

The simulation is done with two lithologies and $\psi_i(b) = \int_0^b k_i(u)du$ with the diffusion coefficients $k_i(b)$ defined by

$$k_i(b) = \begin{cases} k_{i,m} & \text{if } b \leq -\beta, \\ \left(\frac{k_{i,c}}{k_{i,m}}\right)^{\frac{b}{2\beta}} \left(k_{i,c}k_{i,m}\right)^{\frac{1}{2}} & \text{if } -\beta < b < \beta, \\ k_{i,c} & \text{if } b \geq \beta, \end{cases} \tag{19}$$

for $i = 1, 2$, with $k_{1,c} = 10^5$ m^2/yr, $k_{1,m} = 10^4$ m^2/yr, $k_{2,c} = 5.10^4$ m^2/yr, $k_{2,m} = 10^3$ m^2/yr, and $\beta = 1$ m.

The sediment supply is given by the input total flux $\varphi = 2\,m^2/yr$ and the fractional flows $\bar{\mu}_1 = \bar{\mu}_2 = 0.5$ at $x = 0$, and the total output flux φ is set to zero at $x = L_b$. The basin initial composition is $c_1^0(x,z) = c_2^0(x,z) = 0.5$ on the domain $z < h^0(x)$, $x \in \Omega$.

The stratigraphic layers of the basin at time T are defined as the isotime surfaces of the function

$$\mathcal{SL}(x,t,T) = \min_{t \leq t' \leq T} h(x,t'),\ (x,t) \in \mathcal{D},$$

where the minimization over the interval (t,T) accounts for the erosion of the layers between the times t and T.

The mesh is uniform of step Δx. The time stepping is adaptively computed as follows. We fix an objective maximal variation of the sediment thickness Δh_{max} as well as a maximal variation ΔH_m of H_m, a maximal time step Δt_{max}, and an initial time step Δt_0. Then, the successive time steps are computed by the following induction formula:

$$\begin{cases} \Delta t^0 & = \Delta t_0, \\ \Delta t^{n+1} & = \min\Big(\alpha\, \Delta t^n, \Delta t_{max}, \Delta t_m, \frac{\Delta h_{max} \Delta t^n}{(\max_{\kappa \in \mathcal{K}} |h_\kappa^n - h_\kappa^{n-1}|)}\Big) \end{cases} \tag{20}$$

with $\alpha > 1$, and Δt_m such that $|H_m(t^n + \Delta t_m) - H_m(t^n)| = \Delta H_m$.

In case of non convergence of the Newton algorithm after a fixed maximum number of iterations, the time step is restarted with a twice smaller value.

Figure 6 illustrates the influence of the maximum erosion rate parameter E on the stratigraphic layers and the sediment concentration c_1 for $x = 100$ km. This effect is very noticeable for decreasing sea level sequences. For E large, the erosion rate constraint is not active and the continental topography is close to an horizontal straight line at the sea level (for large non-marine diffusion coefficients $k_{i,c}$). On the contrary, for E small, the non-marine erosion is constrained by the maximum erosion rate resulting in a much smoother continental topographical curve down to the sea level.

Note also, as illustrated on the bottom picture of figure 6, that the sediment concentrations may exhibit jumps resulting from erosion followed by sedimentation sequences.

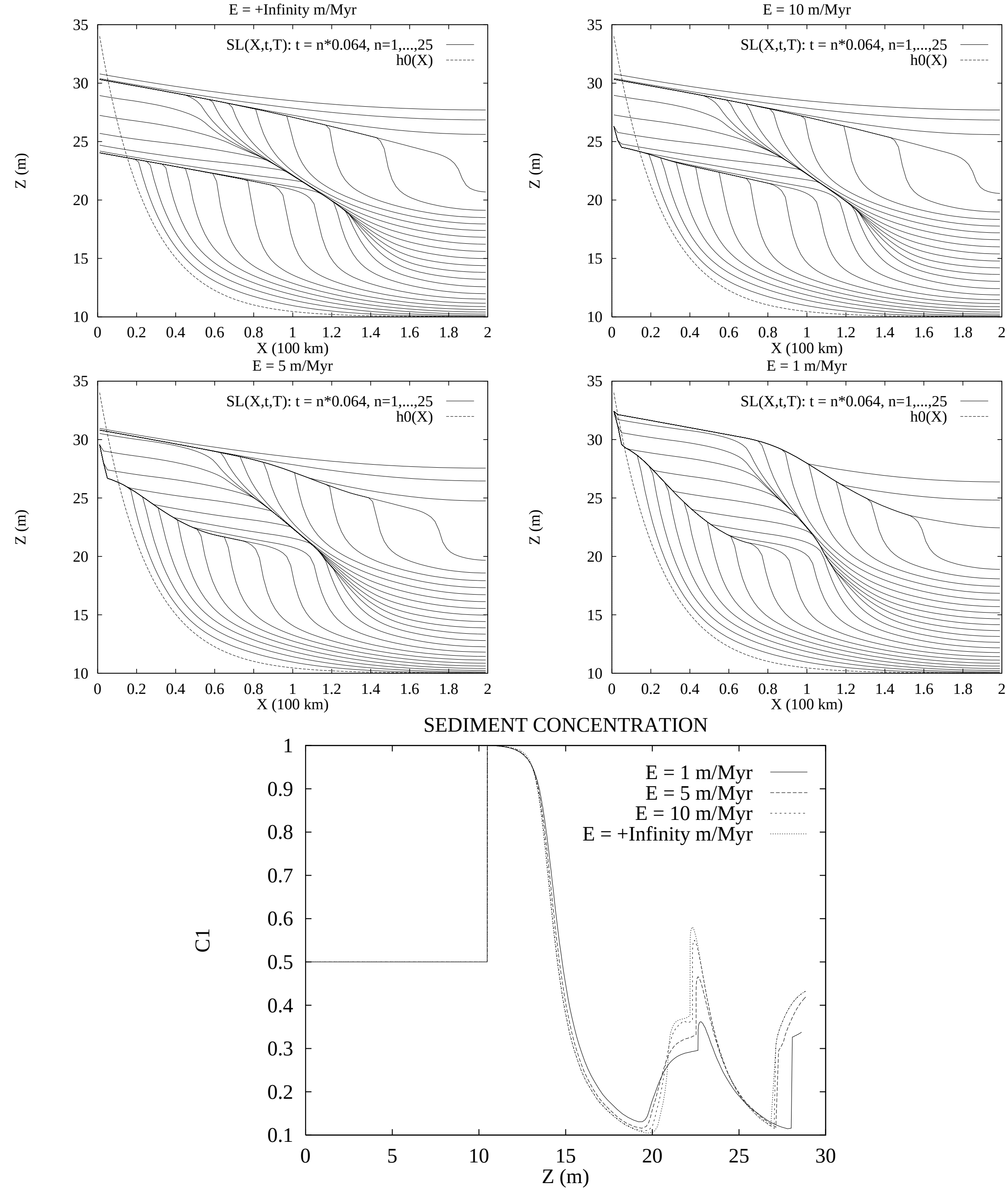

Figure 6: Stratigraphic layers of the basin at time $T = 1.6$ Myr, and sediment concentrations $c_1(x, z, T)$, $x = 100$ km, for the Delta progradation test case with maximum erosion rates $E = 1, 5, 10$, and $+\infty$ m/Myr. The simulation is performed over a time span of 1.6 Myr, with a uniform time step $\Delta t = 0.0025$ Myr, and the mesh size $\Delta x = 2$ km.

The next figure 7 exhibits the plots of the sediment thickness h, the limitor λ, the total flux $\mathbf{f} := \sum_{i=1}^{L} \mathbf{f}_i$, the accumulation rate $\partial_t h$, and the surface sediment concentration c_1^s at times $t = 0.5$ Myr and $t = 0.75$ Myr. It illustrates the discontinuity of the limitor λ at the transition from weather limited to diffusive transport processes, resulting in slope breaks of the sediment thickness.

The total flux $\mathbf{f}$ satisfies the constraint div$\mathbf{f} \leq E$. In one dimension $d = 1$, it results that the total flux slope cannot exceed E which is clearly illustrated on the plots of figure 7.

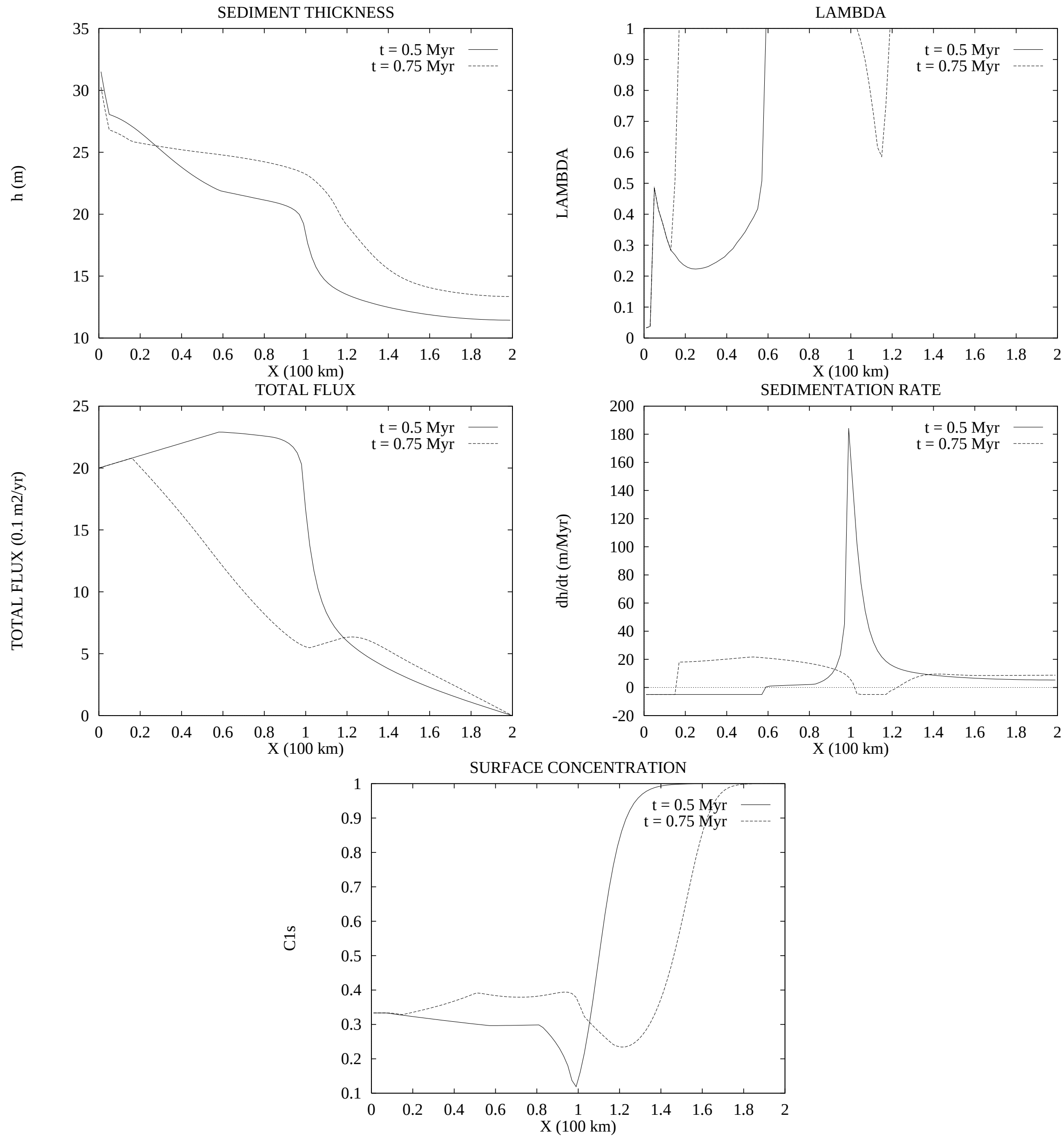

Figure 7: Sediment thickness h, limitor λ, total flux $\sum_{i=1}^{L} \mathbf{f}_i$, sedimentation rate $\partial_t h$, and surface sediment concentration c_1^s, at times $t = 0.5$ and $t = 0.75$ Myr, for the Delta progradation test case with maximum erosion rate $E = 5$ m/Myr, a uniform time step $\Delta t = 0.0025$ Myr, and the mesh size $\Delta x = 2$ km.

Table 1 exhibits the performance of the Newton solver. The number of Newton iterations appears sensitive to the mesh size. Various stabilizations of the algorithm for very large meshes using Quasi Newton techniques or additional diffusion terms will be presented in a forthcoming paper.

Δx	2 km	1 km	0.5 km	0.25 km	0.125 km
Nnew / NΔt / Nfail	720/160/0	1003/160/0	1154/160/2	1434/160/3	2103/164/14

Table 1: Total number of Newton iterations/number of time steps/number of time step failures, for the Delta Progradation test case with maximum erosion rate $E = 1$ m/Myr, and different mesh sizes Δx. The initial and maximum time step is fixed to $\Delta t_0 = \Delta t_{max} = 0.01$ Myr, and $\Delta h_{max} = \Delta H_m = +\infty$, $\alpha = +\infty$. The maximum number of Newton iterations is 25, and the stopping criteria prescribes a relative residual lower than 10^{-5} in l^2 norm.

4.3 Weather limited erosion of an island

We consider the square domain $\Omega = (0, L_b) \times (0, L_b)$ with $L_b = 20$ km. The sea level is fixed to $H_m = 10$ m, and the initial sediment thickness is set to $h^0(x_1, x_2) = 2\,\mathrm{e}^{2-(\frac{x_1}{2L_b}-1)^2-(\frac{x_2}{2L_b}-1)^2}$. The simulation is still done with two lithologies with diffusion coefficients given by (19) with $k_{1,c} = 10^3$ m^2/yr, $k_{1,m} = 2.10^2$ m^2/yr, $k_{2,c} = 5.10^2$ m^2/yr, $k_{2,m} = 50$ m^2/yr, and $\beta = 0$ m.

The sediment fluxes at the boundary $\partial\Omega$ are set to zero and the basin initial composition is given by $c_1^0(x, z) = 1 - c_2^0(x, z) = 0.7$ on the domain $z < h^0(x)$, $x \in \Omega$. The maximum erosion rate is fixed to $E = 5$ m/Myr

The mesh and the time stepping are uniform of sizes $\Delta x_1 = \Delta x_2 = 0.4$ km, and $\Delta t = 0.05$ Myr, and the simulation is performed over a time span of 1 Myr.

The sediment thickness solutions displayed Figure 8 illustrate the coupling between the dependence on the bathymetry of the diffusion coefficients $k_i(b) = \frac{d\psi_i}{db}(b), i = 1, 2$ and the weather limited model. We can observe, in particular on the bottom picture, that the topography under the sea level results from a diffusive dominated transport with low marine diffusion coefficients, whereas the island is eroded under a weather limited mechanism.

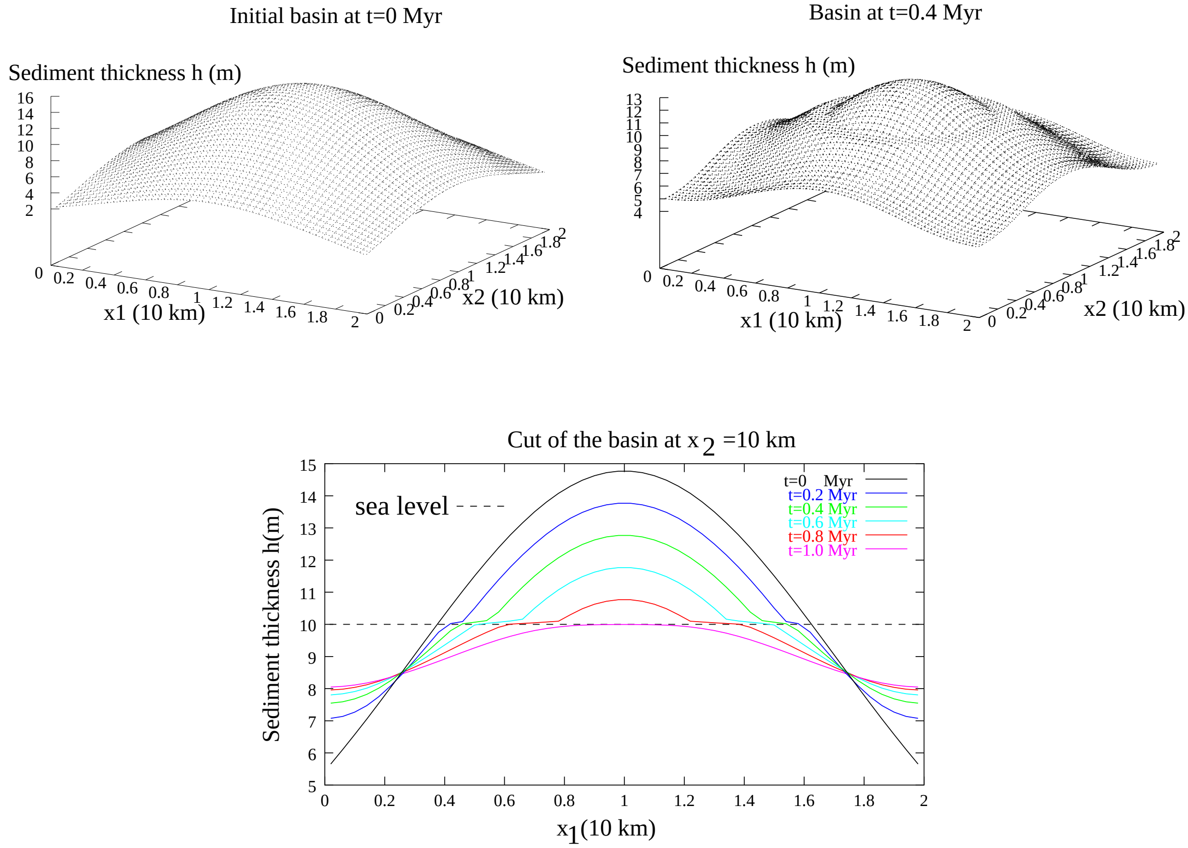

Figure 8: Initial sediment thickness at time $t = 0$, sediment thickness solution at time $t = 0.4$ Myr, vertical 2D cut at $x_2 = 10$ km of the sediment thickness solutions at times $t = 0$, 0.2, 0.4, 0.6, 0.8 and 1 Myr.

5 Conclusion

Large scale mass conservation PDE models have become a powerful tool in the field of stratigraphic basin simulation to investigate the effects of eustasy, tectonics, and sediment supply on facies distribution and stratal geometry of basins. In the petroleum industry these models have been successfully used to reconstruct the history of 3D basins. This is achieved by inversion of the parameters of the direct simulation, (input fluxes, sea level variations, tectonics displacements, diffusion coefficients, and erosion rate), given sediment thickness seismic data and bathymetry and sediment concentrations log data [GJD98], [GJ99].

We have introduced in this paper a new mathematical formulation for the coupling of weather limited erosion and the multi-lithology diffusion models existing only at the discrete level so far. Both the multi-lithology and the coupled models appear as non standard formulations that remains to be analysed mathematically.

It has allowed the definition of a finite volume discretization scheme with implicit time integration which can be proved to be stable. This new scheme is computationally more efficient than existing explicit schemes and enable the use of much larger time steps and meshes. This computational efficiency and the better understanding of the coupled model will be helpful for a more efficient solution of the inverse problem.

A convergence analysis of the discrete scheme in a simplified case [EGGM03] as well as the design of efficient non linear and linear solvers for large 3D basin models will be the subject of forthcoming papers.

Acknowledgements

The authors are thankful to Professors R. Glowinski from the University of Houston, and G. Gagneux from l'Universit de Pau et des Pays de l'Adour for fruitful discussions during the elaboration of this work, and to Vronique Gervais from IFP for the numerical test in 3D.

References

[AH89] R. S. Anderson, N. F. Humphrey, "Interaction of Weathering and Transport Processes in the Evolution of Arid Landscapes", in Quantitative Dynamics Stratigraphy, T.A. Cross, ed., Prentice Hall, pp. 349-361, 1989.

[EGGM03] R. Eymard, T; Gallouët, V. Gervais, R. Masson, "Convergence of a Numerical Scheme for Stratigraphic Modeling", submitted to SIAM J. Numer. Analysis, april 2003.

[EGH00] R. Eymard, T. Gallouët, R. Herbin, "The Finite Volume Method", Handbook of Numerical Analysis, P.G. Ciarlet, J.L. Lions editors, Elsevier, **7**, p. 715-1022, 2000.

[GLT76] R. Glowinski, J.L. Lions, R. Trmolire, "Analyse Numérique des Inéquations Variationnelles", J.L. Lions Editeur, Bordas, paris 1976, T1 et 2.

[G97] D. Granjeon, "Modlisation stratigraphique dterministe; conception et applications d'un modle diffusif 3D multilithologique", Ph. D. dissertation. Gosciences Rennes, Rennes, France, 189 p., 1997.

[GJD98] D. Granjeon, P. Joseph, B. Doligez, "Using a 3-D stratigraphic model to optimise reservoir description", Hart's Petroleum Engineer International, November 1998, p. 51- 58.

[GJ99] D. Granjeon, P. Joseph, "Concepts and applications of a 3D multiple lithology, diffusive model in stratigraphic modelling". In J.W. Harbaugh. and al. (eds.), Numerical Experiments in Stratigraphy, SEPM Sp. Publ. 62, 1999.

[QAD00] A. Quiquerez, P. Allemand, G. Dromart "DIBAFILL: a 3D two lithology diffusive model for basin infilling", Computer and Geosciences, **26**, pp. 1029-1042, 2000.

[R92] Jan C. Rivenaes, "Application of a dual lithology, depth-dependent diffusion equation in stratigraphic simulation", Basin Research **4**, pp. 133-146, 1992.

[R97] Jan C. Rivenaes, "Impat of Sediment transport efficieny on large-scale sequence arhitecture: results from stratigraphic computer simulation", Basin Research **9**, pp. 91-105, 1997.

[TH89] D.M. Teztlaff, J.W. Harbaugh, "Simulating Clastic Sedimentation", Van Norstrand Reinhold, New York, 1989.

[TS94] G. E. Tucker, R. L. Slingerland, “Erosional dynamics, flexural isostasy, and long-lived escarpments: A numerical modeling study”, J. of Geophysical Research, Vol **99**, B6, pp. 12,229-12,243, june 10, 1994.